High-yield, single-step separation of metallic and semiconducting SWCNTs using block copolymers at low temperatures

Homenick, Christa M.; Rousina-Webb, Alexander; Cheng, Fuyong; Jakubinek, Michael B.; Malenfant, Patrick R. L.; Simard, Benoit

Publisher's version / Version de l'éditeur:
https://doi.org/10.1021/jp5030476
The Journal of Physical Chemistry C, 118, 29, pp. 16156-16164, 2014-06-03

THE JOURNAL OF PHYSICAL CHEMISTRY C

Article

pubs.acs.org/JPCC

High-Yield, Single-Step Separation of Metallic and Semiconducting SWCNTs Using Block Copolymers at Low Temperatures

Christa M. Homenick,*[,†] Alexander Rousina-Webb,[†] Fuyong Cheng,[†] Michael B. Jakubinek,[†] Patrick R. L. Malenfant,[‡] and Benoit Simard*[,†]

[†]Security and Disruptive Technologies Portfolio, National Research Council Canada, 100 Sussex Drive, Ottawa, Ontario K1A 0R6, Canada

[‡]Security and Disruptive Technologies Portfolio, National Research Council Canada, M-50, 1200 Montreal Road, Ottawa, Ontario K1A 0R6, Canada

ABSTRACT: Electronic type separation of SWCNT material is necessary to facilitate the development of carbon nanotube electronics. A convenient, high-yield, single-step separation of metallic and semiconducting SWCNTs has been developed using block copolymers and density gradient ultracentrifugation. In particular by varying the centrifugation temperature and dissolved oxygen content under acidic conditions, extraction efficiencies of up to 65% were achieved with both metallic and semiconducting SWCNT electronic purity exceeding 99% as determined by absorption spectroscopy. It was demonstrated that lowering the temperature during the DGU separation, which is expected to increase the difference in densities between metallic and semiconducting nanotube complexes, results in higher purity and yield. Semiconducting and metallic bands are separated simply with a disposable pipet such that specialized fractioning equipment is not required for effective isolation of enriched SWCNTs.

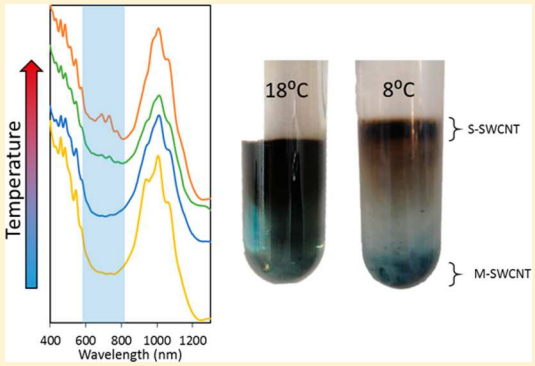

Single-walled carbon nanotubes (SWCNTs) have shown great potential for application in nanoelectronic devices such as individual SWCNT transistors,[1,2] thin-film transistors,[3−5] and sensors.[6−9] Due to the nonselective nature of the established synthetic methods for SWCNTs, which yield both metallic and semiconducting SWCNTs, the performance of nanoelectronic devices is significantly hindered. Although significant progress has been made toward selective chiral synthesis,[10,11] a standard, high-yield process is not yet available. As a result, electronic type separation is necessary to facilitate the development of these applications with SWCNTs.

Separations of this nature have been explored extensively through a variety of techniques including dielectrophoresis,[12−14] DNA wrapping,[15−17] phase separation,[18] polymer wrapping,[19−25] chromatography,[17,26−29] and density gradient ultracentrifugation (DGU).[30−32] DGU is one of the more widely used methods for electronic type and specific chirality separation.[33] Effective DGU separation relies on the differences in buoyant density between surfactant complexes as the intrinsic density of SWCNTs themselves vary little with chirality.[34] Certain surfactants have been found to interact differently with semiconducting and metallic SWCNTs.[31] This selectivity is exploited through the use of various cosurfactant mixtures to create surfactant-encapsulated SWCNTs of varying density, according to helicity. The mixture of SWCNTs is then subjected to high centripetal force in the presence of a density gradient, resulting in movement of SWCNTs to their respective isopycnic points. The SWCNTs are then isolated by fractionation. Extensive screening has shown that there are a limited number of surfactants that demonstrate the required interactions necessary for electronic-type separation.[35]

Recently, Antaris et al.[36] have demonstrated DGU separation of SWCNTs using a class of nonionic biocompatible block copolymers known as Pluronic, an ABA block copolymer consisting of a central chain of hydrophobic poly(propylene oxide) (PPO) surrounded on either side by hydrophilic poly(ethylene oxide) (PEO). The central hydrophobic block interacts with SWCNTs while the outer hydrophilic blocks allow for dispersion in aqueous media. These surfactants have been used to prepare concentrated aqueous dispersions of SWCNTs.[37,38] Furthermore, the interaction of these polymers with SWCNTs[39−43] and the mechanism by which electronic separation occurs[44] has been studied. However, separations thus far suffer from many of the same drawbacks as traditional DGU; namely, low yield, optimization for a single electronic type, and the requirement of specialized fractioning equipment to achieve effective separation.

The role of temperature on DGU-based separation methods for SWCNTs has received limited attention. Yanagi et al. developed a theoretical framework linking the temperature of a DGU separation to the buoyant density of SWCNT−surfactant complexes.[45] At temperatures below 10 °C, excessive solution

Received: March 27, 2014
Revised: May 28, 2014
Published: June 3, 2014

dx.doi.org/10.1021/jp5030476 | J. Phys. Chem. C 2014, 118, 16156−16164

viscosity and crystallization of the gradient medium limited SWCNT separations.[45] The effect of temperature, however, is still a relatively unexplored area in relation to DGU-based separations of SWCNTs, and the benefits of tuning this parameter have yet to be fully demonstrated. The iodixanol/Pluronic DGU system should be advantageous for investigating the role of temperature on the separation of SWCNTs, as challenges resulting from solubility/crystallization of the surfactant and density gradient media are avoided at reduced temperatures.

Herein we present a convenient, high-yield, single-step DGU separation method to obtain both metallic and semiconducting SWCNTs. Improved separation and yield were realized by reducing the separation temperature and increasing dissolved oxygen (DO) content under acidic conditions. Utilizing Pluronic as a dispersant for SWCNTs enabled DGU separations at temperatures below 10 °C, which resulted in extraction yields of up to 65% and purity in excess of 99% for both metallic and semiconducting SWCNT. This SWCNT separation method was capable of electronic type enrichment regardless of the synthetic method used to produce the SWCNTs and their respective impurities. Furthermore, this method was capable of exceeding 2 mg/mL loading of raw SWCNTs and does not require specialized fractionation equipment. As a result of these features, this enrichment methodology will help expand the accessibility of highly enriched semiconducting and metallic SWCNTs.

RESULTS AND DISCUSSION

Pluronic F108 and F68 were selected as DGU surfactants for dispersion of SWCNTs. Pluronic F108 (PEO_{132}–PPO_{50}-PEO_{132}) and F68 (PEO_{76}–PPO_{29}–PEO_{76}) both contain the same ratio of PPO to PEO with the key difference being molecular weight of the polymer. Pluronic F108 has a molecular weight of 14600 g/mol, whereas F68 has a much smaller molecular weight of 8400 g/mol. SWCNTs synthesized by either arc discharge,[46] laser ablation,[47] or plasma torch[48] were dispersed in 1% w/v Pluronic surfactant and processed to minimize bundling.

As seen by optical absorption spectroscopy, the resulting F68/SWCNT and F108/SWCNT dispersions did not vary with respect to SWCNT diameter or chirality as a result of the Pluronic used (Figure 1). By examining the SWCNT spectra more closely, differences in the dispersions were evident. The normalized F68/SWCNT absorption spectrum is slightly red-shifted when compared to the corresponding F108/SWCNT spectrum. In addition, the features in the F68/SWCNT spectrum were broader than those of the F108/SWCNT sample. A red shift and broadening of the absorption features has been attributed to an increase in self-assembly (bundling) of SWCNTs in dispersions.[49−51] Furthermore, the intensity of the F68/SWCNT dispersion spectrum was greater between 400 and 900 nm. Similar increases in intensity have been attributed to increased background absorption as a result of spectral congestion due to bundling.[51] Lastly, Pluronic F108 dispersed 1.6 times arc discharge, 1.9 times laser ablation, and 2.0 times plasma torch SWCNTs at the same surfactant loading as F68.

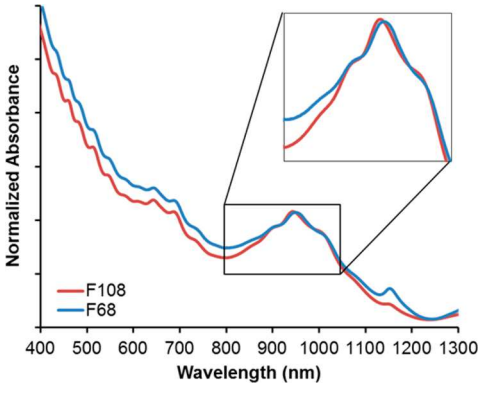

Figure 1. Visible/NIR absorption spectra of plasma torch SWCNTs dispersed in Pluronic F68 and F108. Spectra have been normalized to the highest intensity peak in the S_{22} region. The features near 1150 nm are uncompensated absorptions from water vapor.

While individualized SWCNTs are critical for effective DGU separation by electronic type, the surfactant concentration also plays a key role in realizing effective separation.[36] Pluronic surfactants do not form micelles at a specific critical micelle concentration but rather over a concentration range commonly referred to as the aggregation concentration range.[52,53] When Pluronic/SWCNT dispersions were mixed with iodixanol, a self-forming density gradient medium, as part of the DGU preparation, the surfactant concentration was consequently diluted from 1% w/v to 0.44% w/v. While a F108 concentration of 0.44% w/v was sufficient to maintain the SWCNTs in solution, this concentration was too low for F68 dispersion, which resulted in flocculation of SWCNTs during ultracentrifugation. This phenomenon is indicative of a dynamic polymer equilibrium, with instantaneous surface coverage not being sufficient to prevent bundling at high centripetal forces.[36] To address this issue, 1% w/v F68 was added to the density gradient media so the Pluronic concentration would be maintained at 1% w/v after the F68/SWCNT dispersion was combined with the density gradient media. DGU separations were found to be optimal at concentrations of 0.44% w/v for F108 and 1% w/v for F68, which were well within the necessary aggregation concentration ranges.[52,54]

Following ultracentrifugation at pH 3, broad banding regions were observed along the centrifuge tubes, with gradients in color from brown/red at the top to deep blue/green at the very bottom (Figure 2 and Figure 3). The bands were separated into 100 μL fractions and characterized by optical absorption spectroscopy to estimate the degree of electronic enrichment. The top bands (dark brown/red) contained the highest purity semiconducting SWCNTs, with enrichment decreasing as the distance from the top of the centrifuge tube increased. High purity metallic SWCNTs are found at the bottom of the centrifuge tubes, seen distinctly as blue/green in color. The S_{22} and M_{11} transitions can be observed in the absorption spectra and were used to evaluate the degree of electronic enrichment.[36,55,56] Specifically, the semiconducting enrichment was calculated as a percentage of the baseline corrected area of the S_{22} peak divided by the sum of the baseline corrected S_{22} and M_{11} peak areas.[36] Extraction yields were calculated through use of optical absorbance spectra taken before and after the separation process. The baseline-corrected areas under the S_{22} transitions were normalized to the fraction volume and relevant dilution. The extraction efficiency is defined as the ratio of the area of the S_{22} peak in the analyzed fraction to its area in debundled SWCNT solution pre-DGU.[36]

dx.doi.org/10.1021/jp5030476 | J. Phys. Chem. C 2014, 118, 16156−16164

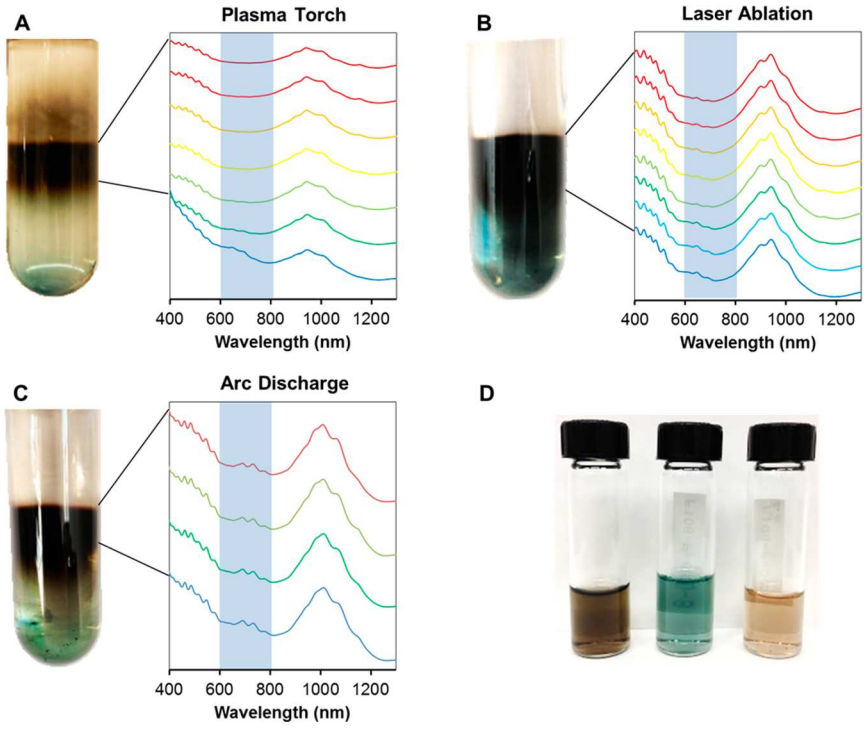

Figure 2. DGU-based separations of SWCNTs using Pluronic F108 performed under acidic conditions at 18 °C for (A) plasma torch, (B) laser ablation, and (C) arc discharge grown SWCNTs. The highest purity fractions (D) were combined for analysis: (left) unsorted SWCNTs, (middle) metallic enriched, (right) semiconducting enriched, for laser ablation grown SWCNTs.

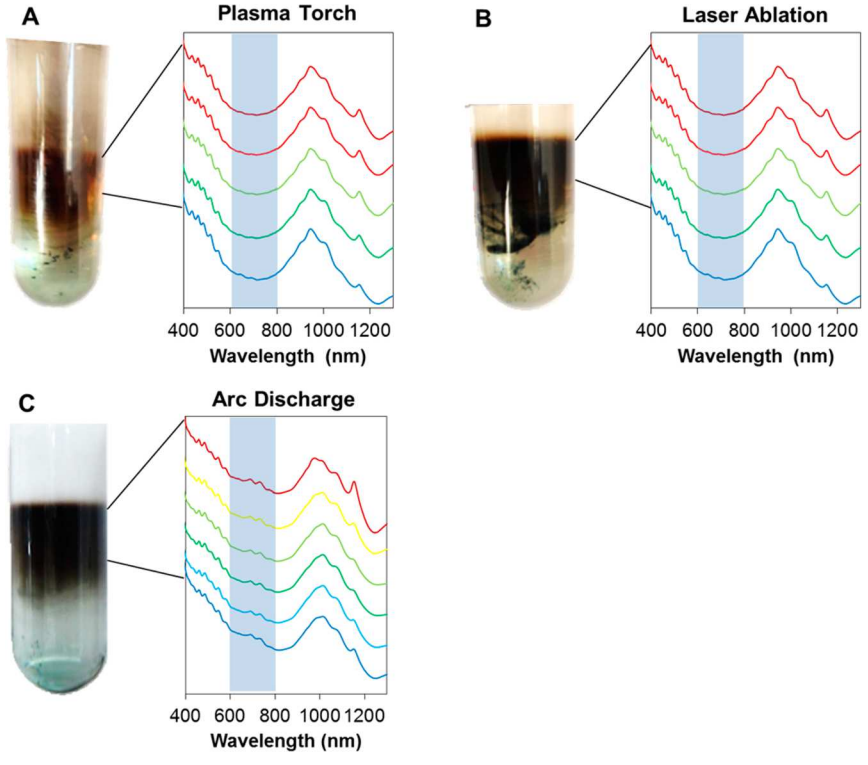

Figure 3. DGU-based separations of SWCNTs using Pluronic F68 performed under acidic conditions at 18 °C for (A) plasma torch, (B) laser ablation, and (C) arc discharge grown SWCNTs.

Absorption spectra of the separated semiconducting fractions are shown in Figures 2 and 3. For all SWCNT materials tested, Pluronic F108 allowed for higher semiconducting enrichment and extraction efficiency than that for Pluronic F68 (Table 1). The increased enrichment can be attributed to the higher individualization of SWCNTs in F108, allowing for fewer bundles of mixed electronic type. The weaker surfactant–SWCNT interactions of F68 are seen in the separation of laser

dx.doi.org/10.1021/jp5030476 | J. Phys. Chem. C 2014, 118, 16156–16164

Table 1. Tabulated Maximum Obtained Semiconducting Purity and Respective Extraction Efficiency for DGU-Processed Samples

Pluronic	synthesis method	maximum SWCNT enrichment (metallic:semiconducting)	maximum SWCNT enrichment (% semiconducting)	extraction efficiency at maximum purity (%)
F108	arc discharge	0.037	96	13
	laser ablation	0.0039	>99	13
	plasma torch	0.0014	≫99	12
F68	arc discharge	0.024	>97	11
	laser ablation	0.0029	>99	3.0
	plasma torch	0.0033	>99	3.2

ablation SWCNTs (Figure 3), where the metallic SWCNTs self-assemble to the point of flocculation, a phenomenon not observed in the F108 separation of the same material. This phenomenon demonstrates the preferential bundling of metallic SWCNTs, thus allowing for metallic (Figure 4) and

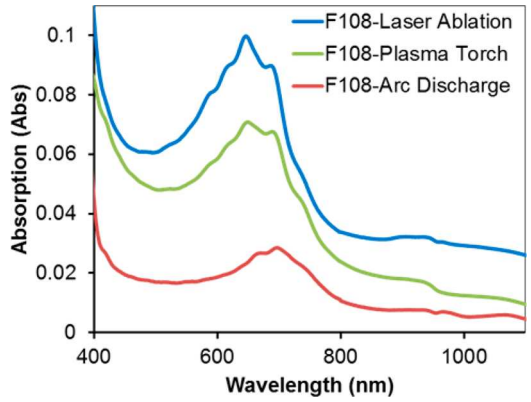

Figure 4. Optical absorption spectra of metallic-enriched SWCNT fractions found at the bottom of the centrifuge tube. Features from 900 to 1100 nm are a result of residual iodixanol from the density gradient.

semiconducting SWCNTs to be isolated at high purity (greater than 99%) and high yield at the same time. The electronic-type enrichment for the metallic SWCNT fraction is estimated at greater than 99% because the S_{22} transition from the semiconducting SWCNTs is not visible and therefore cannot be measured because of the low sensitivity of absorption spectroscopy and error propagation in the method used; 99% represents the assessment limit with this method. The extraction efficiency for the metallic fraction was at least 20%. Metallic SWCNT extraction efficiency was calculated as follows: [(metallic fraction absorbance at 650 nm)(volume of the metallic SWCNT fraction)]/[(unsorted solution absorbance at 650 nm)(volume of SWCNT placed in the centrifuge system)] × 100%. Importantly, F108 was capable of not only higher extraction efficiencies but also higher SWCNTs loadings into the DGU process due to the higher concentration of SWCNTs dispersed by F108 than by F68, thus leading to high throughput.

SWCNTs become reversibly protonated under acidic conditions in the presence of physisorbed oxygen,[57] leaving a negative image charge across the surface of the SWCNT.[58] The doping order is a function of SWCNT electronic properties, with metallic SWCNTs being protonated first, followed by small band gap semiconducting SWCNTs.[57] The presence of physisorbed oxygen plays a key role in this process, controlling both the rate and degree of protonation.[57] The charge localization left on protonated SWCNTs repels the electron-rich methyl groups found on the PPO block of Pluronic, resulting in reduced interactions with these SWCNTs. It has been proposed that this effect causes preferential bundling of metallic SWCNTs, thereby allowing for density-based separation.[59]

At 18 °C, the extraction efficiencies are low due to the close proximity of the metallic and semiconducting bands, which results in significant overlap. A large quantity of the SWCNTs is left partially enriched, with many of the same drawbacks as unsorted material. The material that is highly enriched in semiconducting SWCNTs is difficult to separate due to the small fractions that must be taken and analyzed prior to use.

Motivated by the improved results of using Pluronic F108 and by a mechanistic understanding of the surfactant-based separation, attempts were made to exploit the role of physisorbed oxygen on the process. By increasing the dissolved oxygen content within the system, the doping level of metallic SWCNTs should be increased, promoting further self-assembly and enhancing separation. DGU separation of laser ablation grown SWCNTs in F108 was carried out at 18 °C after bubbling oxygen through the SWCNT/gradient mixture for 1 h prior to ultracentrifugation (Figure 5). The semiconducting

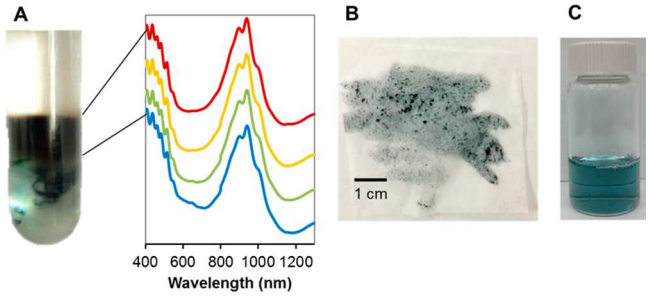

Figure 5. Oxygen-enriched DGU-based separation of laser ablation grown SWCNTs using Pluronic F108. Increased bundling of metallic SWCNTs is seen (A) in the centrifuge tube, resulting in increased semiconducting enrichment as evidenced by the optical absorption spectra. The bundled metallic SWCNTs can be easily filtered out (B) and redispersed under mild bath sonication (C).

band was separated into 0.5 mL fractions and analyzed by optical absorption spectroscopy. Increased bundling of metallic SWCNTs was immediately evident after ultracentrifugation due to the increased flocculation of metallic SWCNTs (Figure 5a). The bundled metallic SWCNTs were easily separated from the metallic dispersion by filtration. The filtered SWCNT material could be fully redispersed in surfactant after only 30 s of bath sonication. The increased bundling of metallic SWCNTs also has a pronounced effect on the enrichment quality and quantity of semiconducting SWCNTs. Increased semiconducting purity

dx.doi.org/10.1021/jp5030476 | J. Phys. Chem. C 2014, 118, 16156−16164

is observed in all fractions, with the M_{11} transition becoming undetectable in the uppermost fractions, indicating a semiconducting purity in excess of 99% (Figure 5). The semiconducting extraction efficiency was increased to 22% due to the increased density of metallic SWCNTs, which increased the separation of the metallic and semiconducting bands. Furthermore, increasing the dissolved oxygen content also decreased bundling in the semiconducting enriched fractions, as seen by a blue shift in the spectrum of the oxygen enriched sample (Figure 6).

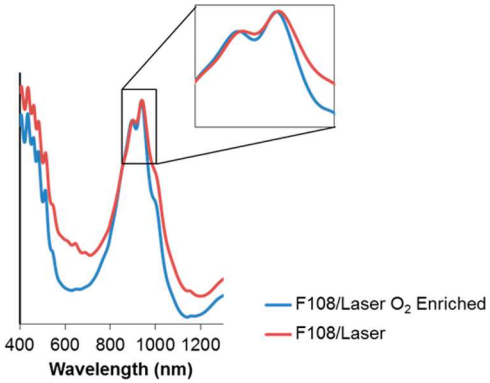

Figure 6. Comparison of the optical absorption spectra of highly enriched semiconducting bands extracted from DGU-based separations of laser ablation SWCNTs in Pluronic F108.

The main issue with separating high-purity metallic and semiconducting SWCNTs in high yield by DGU is the overlapping density regions. Results from Yanagi et al. indicate that by lowering the temperature of separation, the differences in density between SWCNT−surfactant complexes are increased.[45] We present a similar theoretical framework to this idea, but applied from the perspective of Pluronic-encapsulated SWCNTs (Figure 7). First, the model assumes that the density of the metallic, ρ_{metal}, and semiconducting, ρ_{semi}, SWCNT complexes can be written as the sum of the SWCNT densities,[30] ρ_{cnt_m} and ρ_{cnt_s}, and the added density resulting from surfactant encapsulation, ρ_{surf_m} and ρ_{surf_s} (eq 1). In the Pluronic encapsulated system the ρ_{cnt_m} is redefined as the density of the bundled metallic SWCNTs, which do not interact well with Pluronic, and ρ_{cnt_s} is the density of the individualized semiconducting SWCNTs, which do interact well with Pluronic (Figure 7).

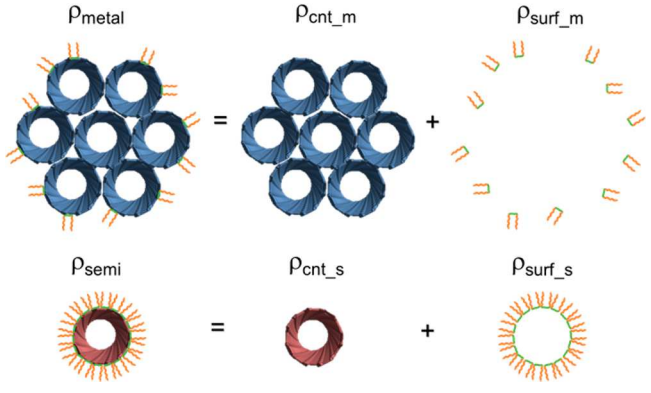

Figure 7. Graphical representation of eq 1 illustrating the breakdown of SWCNT−surfactant complex densities into contributions from SWCNTs and surfactant encapsulation. The metallic SWCNT−surfactant complexes have a significantly larger contribution from SWCNT density compared to semiconducting type, due to their preferentially bundled nature and sparse surfactant contribution when compared to the semiconducting−surfactant complexes.

$$\rho_{metal} = \rho_{cnt\_m} + \rho_{surf\_m}$$
$$\rho_{semi} = \rho_{cnt\_s} + \rho_{surf\_s} \quad (1)$$

To optimize separation, it is obvious that the difference between the density of the metallic and semiconducting complexes must be maximized (eq 2).

$$\rho_{metal} - \rho_{semi} = \rho_{cnt\_m} - \rho_{cnt\_s} + \rho_{surf\_m} - \rho_{surf\_s} \quad (2)$$

Due to the preferential bundling of metallic SWCNTs, under acidic conditions in Pluronic,[59] the density of the bundled metallic SWCNTs can be assumed to be much larger than that for the individualized semiconducting SWCNTs. The added density of surfactant is a function of the concentration of surfactant at the SWCNT surface and the free surfactant in solution (eq 3).[60]

$$X_{metal} = X_1 e^{-\Delta\mu_{metal}/kT}$$
$$X_{semi} = X_1 e^{-\Delta\mu_{semi}/kT} \quad (3)$$

where X_{metal} and X_{semi} are the concentrations of surfactant at the SWCNT surface and are proportional to the added surfactant densities. Here, X_1 is the concentration of free surfactant in solution, k is the Boltzmann constant, and $\Delta\mu$ is the difference in chemical potential between a surfactant molecule in solution and one found at the SWCNT surface. As a result, the ratio of the added density due to surfactant adsorbed to the metallic SWCNTs relative to semiconducting SWCNT surfaces can be written as in eq 4.

$$\frac{\rho_{surf\_m}}{\rho_{surf\_s}} \propto e^{(\Delta\mu_{semi} - \Delta\mu_{metal}/kT)} \quad (4)$$

Therefore, as the temperature of the separation is decreased, the difference in density between the metallic and semiconducting SWCNT complexes due to the surfactant at the SWCNT surface should increase. As shown in Figure 6, this effect is further amplified in the presence of oxygen enrichment, which increases bundling of metallic SWCNTs, thus increasing the metallic density further while simultaneously reducing the density of semiconducting SWCNTs by decreasing their bundling.

To test this hypothesis in a Pluronic dispersion, a series of DGU experiments were carried out at progressively lower temperatures (Table 2). As the temperature decreases, the semiconducting band decreases in width but moves up in the centrifuge tube (Figure 8), while the metallic SWCNTs move closer to the bottom of the centrifuge tube and compress. The density of the metallic SWCNTs is increased enough for them to deposit as solid material on the bottom of the centrifuge tube. The semiconducting purity obtained at 3 °C is higher than any fraction obtained at 18 °C, as the M_{11} transition is lost into the noise in the absorption spectra (Figure 9); it is estimated at greater than 99% with an extraction efficiently of 23−37% depending on SWCNT source material (Figure 10). Unlike previous reports, the separation was not hindered by solution viscosity being too high or crystallization of either iodixanol or Pluronic. While the extraction efficiency is 2−3

dx.doi.org/10.1021/jp5030476 | J. Phys. Chem. C 2014, 118, 16156−16164

Table 2. Tabulated Maximum Obtained Semiconducting Purity and Respective Extraction Efficiency for DGU-Processed Samples as a Function of Temperature

synthesis method	temperature (°C)	maximum SWCNT enrichment (M_{11}:S_{22})	maximum SWCNT enrichment (% semiconducting)	extraction efficiency at maximum purity (%)
arc discharge	18	0.0370	96	13
	13	0.0120	>98	22
	8	0.0012	>99	38
	3	0.0005	≫99	23
laser ablation	18	0.0039	>99	13
	13	0.0029	>99	28
	8	0.0050	>99	44
	3	0.0005	≫99	33
plasma torch	18	0.0014	>99	12
	13	0.0012	>99	47
	8	0.0007	≫99	66
	3	0.0005	≫99	37

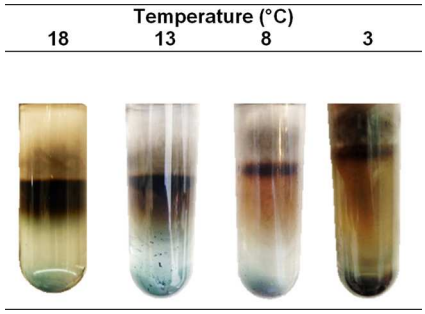

Figure 8. Typical DGU separation of plasma torch SWCNTs at each temperature.

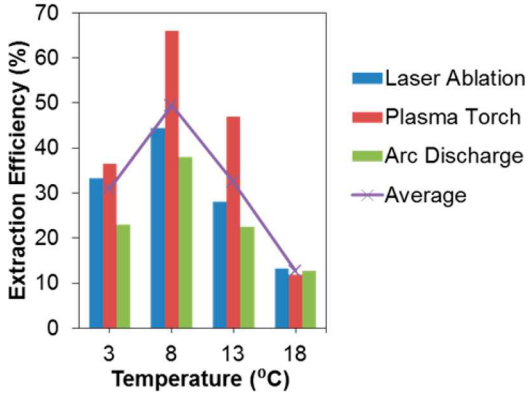

Figure 10. Semiconducting SWCNT extraction efficiency plotted as a function of temperature for Pluronic F108 dispersed laser ablation, plasma torch, and arc discharge SWCNTs separated by DGU.

times higher at 3 °C than at 18 °C, it is 3–6 times higher at 8 °C depending on SWCNT source material but without the same level of enrichment observed at 3 °C (Figure 10). While the semiconducting enrichment is the highest when the separation is performed at 3 °C, the yield actually diminishes from separations performed at 8 °C. It is hypothesized that at 3 °C there may not only be bundled metallic SWCNTs being separated from semiconducting SWCNTs but now more significant separation of different diameter or bundled semiconducting SWCNTs as evident by the streaking of the semiconducting band in the DGU tube (Figure 8) and a change in the S_{22} peak shape (Figure 9). Furthermore, the surfactant concentration on the tube surface will also decrease as temperature is reduced, allowing semiconducting SWCNTs to bundle, which causes the semiconducting band to be more dispersed (Figure 8).

Lowering the temperature increases the maximum amount of dissolved oxygen present in the system,[61] increasing the bundling of metallic SWCNTs. This effect is consistent with the improved separation observed here when the DGU mixture was bubbled with oxygen prior to separation. Lower temperature also decreases the rate of adsorption/desorption of surfactant on the SWCNT surface,[57] lowering instances of

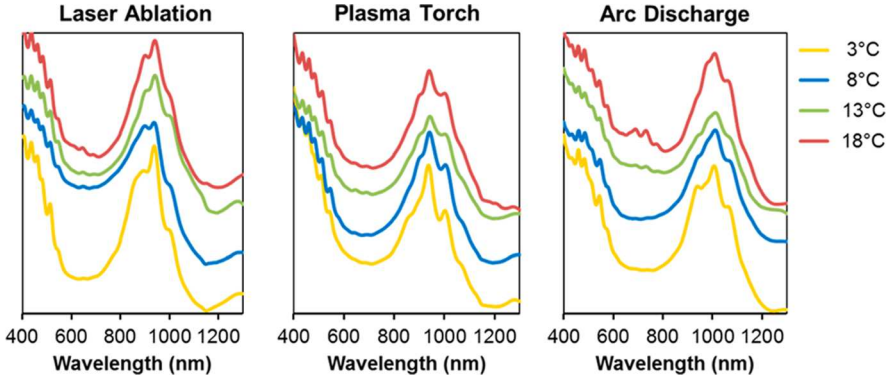

Figure 9. Normalized optical absorption spectra of highly enriched semiconducting band extracted from DGU-based separations laser ablation, plasma torch, and arc discharge SWCNTs at 3 °C, 8 °C, 13 °C, 18 °C. The semiconducting enrichment at 3 °C is higher than any fractions obtained at 18 °C, with metallic transitions no longer visible in some samples.

dx.doi.org/10.1021/jp5030476 | J. Phys. Chem. C 2014, 118, 16156–16164

bundling under high centripetal force. These findings suggest a possible explanation for the semiconducting enrichment dependence on the SWCNT production source at 18 °C. Arc discharge SWCNTs have a mean diameter larger than that of either plasma torch or laser ablation grown SWCNTs. The van der Waals coefficient of SWCNTs increase as a function of diameter,[62] therefore suggesting increased $\pi-\pi$ interactions and subsequent bundling for SWCNTs produced by an arc discharge synthesis. As a result of this poor individualization, enrichment is hampered for arc discharge SWCNTs at 18 °C. Furthermore, the plasma torch SWCNTs contained more amorphous carbon impurities than the other SWCNT sources, which facilitates the individualization of the SWCNTs by preventing their self-assembly. The amorphous carbon in the plasma torch SWCNT material is evident in the DGU separation as the black band above the deep red semiconducting SWCNT band (Figure 8). Because individualization is increased at lower temperatures, the magnitude of enrichment is much greater.

■ CONCLUSIONS

High-yield, single-step separation of metallic and semiconducting SWCNTs was demonstrated using temperature-controlled DGU in Pluronic-based dispersions. It was demonstrated that lowering the temperature of the DGU separation resulted in higher purity and yield. The presence of dissolved oxygen was shown to play a key role in realizing effective separation. Semiconducting and metallic bands are separated simply with a pipet such that specialized fractioning equipment is not required for effective isolation of enriched SWCNTs. This enrichment method provides a simple way to significantly boost yield without sacrificing purity using a new protocol that is universally applicable to three large diameter tube types and can be easily implemented as a drop-in solution for all researchers currently using DGU.

■ EXPERIMENTAL SECTION

General. SWCNTs were purchased from Carbon Solutions (arc discharge synthesis) and Raymor Industries Inc. (plasma torch synthesis). SWCNTs were synthesized at the National Research Council of Canada by a laser ablation synthesis method.[47] Pluronic F108 (poly(ethylene oxide)$_{132}$-*b*-poly(propylene oxide)$_{50}$-*b*-poly(ethylene oxide)$_{132}$) and F68 (poly(ethylene oxide)$_{76}$-*b*-poly(propylene oxide)$_{29}$-*b*-poly(ethylene oxide)$_{76}$) were provided by BASF for research and development. All other reagents were purchased from Aldrich and used as received. Optical absorption spectroscopy was performed using a UV−vis/NIR Varian Cary 5000 spectrophotometer, which was purged with nitrogen gas. Ultrasonication was performed using a Mixonix Ultrasonic Liquid Processor equipped with a 1/8 in. tapered horn tip. Centrifugation was performed using a Thermo Scientific Sorvall Legend XIR centrifuge. Ultracentrifugation was performed using a Beckman Coulter Optima L-90K centrifuged equipped with a 70 Ti rotor. A Fischer Scientific Accumet Research AR15 pH meter was used to measure pH.

Pluronic Dispersions of SWCNTs. SWCNT dispersions (1 mg/mL) were prepared by dispersing 35 mg of as received SWCNTs in 35 mL of a 1% w/v solution of Pluronic F108 or F68 by horn sonication utilizing a duty cycle of 50% at 30% of the maximum amplitude for 1 h. The SWCNT mixture was submersed in an ice bath for the duration of sonication to reduce heating. The dispersion was subsequently centrifuged at 15 000 *g* and 18 °C for 1 h to remove large SWCNT bundles. Following centrifugation, the upper 75% of the solution was carefully removed by Pasteur pipet. To further minimize bundling of SWCNTs in solution, the dispersion was then ultracentrifuged at 279 000*g* and 18 °C for 1 h. Again the uppermost 75% of supernatant was removed and used directly for DGU processing. At a 1% w/v Pluronic loading, 1% and 2% of the raw SWCNT source materials were recovered as dispersed nanotubes for F68 and F108 dispersions, respectively.

DGU-Based Separation of SWCNTs Using Pluronic F108/SWNT Dispersions. SWCNTs dispersed in 1% w/v Pluronic F108 were added to a 60% w/v solution of iodixanol, a density gradient medium (DGM). Volumes were adjusted to final concentrations of 33% w/v and 0.44% w/v of iodixanol and Pluronic F108, respectively. The solution pH was then adjusted to 3 using 0.1 M HCl while under constant stirrring. The mixture was then homogenized by ultrasonication for 10 min with a duty cycle of 50% at 30% of the maximum amplitude. The resulting homogeneous SWCNT-DGM solutions were subsequently ultracentrifuged at 230 000*g* for 24 h at 18 °C, 13 °C, 8 °C, or 3 °C. Samples were stored at room temperature prior to ultracentrifugation.

DGU-Based Separation of SWCNTs Using Pluronic F68/SWNT Dispersions. Similar to above, SWCNTs dispersed in 1% w/v Pluronic F68 were added to a 60% w/v solution of iodixanol. Volumes were adjusted to final concentrations of 33% w/v and 1.0% w/v of iodixanol and Pluronic F68, respectively. The solution pH was then adjusted to 3 using 0.1 M HCl while under constant stirring. The mixture was then homogenized by ultrasonication for 10 min with a duty cycle of 50% at 30% of the maximum amplitude. The resulting homogeneous SWCNT-DGM solutions were subsequently ultracentrifuged at 230 000*g* for 24 h at 18 °C, 13 °C, 8 °C, or 3 °C. Samples were stored at room temperature prior to ultracentrifugation.

DGU-Based Separation of SWCNTs Using Oxygen-Enriched Pluronic F108/SWNT Dispersions. A 100 mL round-bottom flask was charged with the Pluronic F108/SWNT/iodixanol mixture after it was homogenized. The flask was subsequently purged with oxygen gas for 1 h. The resulting oxygen-enriched solution was subsequently transferred into a sealed centrifuge tube using a cannula and positive pressure. The solution was then immediately ultracentrifuged at 230 000*g* for 24 h and 18 °C.

Fractionation and Characterization of Samples. Samples were fractioned while still cold, immediately following ultracentrifugation. Solutions ultracentrifuged at 18 °C and 13 °C were fractioned into 100−500 μL slices using a micropipet. Samples performed at lower temperatures were fractioned by directly pipetting isolated bands in aliquots of approximately 1.5 mL. Fractions were diluted to 3 mL with corresponding 1% w/v Pluronic solution and characterized by optical absorption spectroscopy. Semiconducting SWCNT enrichment and extraction efficiency was estimated using a previously report method.[36] Metallic SWCNT extraction efficiency was calculated as follows: [(metallic fraction absorbance at 650 nm)(volume of the metallic SWCNT fraction)]/[(unsorted solution absorbance at 650 nm)(volume of SWCNT placed in the centrifuge system)] × 100%.

dx.doi.org/10.1021/jp5030476 | J. Phys. Chem. C 2014, 118, 16156−16164

AUTHOR INFORMATION

Corresponding Authors

*Phone: (613) 991-3845, fax: (613) 991-2648, e-mail: Christa.Homenick@nrc-cnrc.gc.ca.

*Phone: 613-990-0977, fax: 613-991-2648, e-mail: Benoit.Simard@nrc-cnrc.gc.ca.

Notes

The authors declare no competing financial interest.

REFERENCES

(1) Javey, A.; Guo, J.; Wang, Q.; Lundstrom, M.; Dai, H. Ballistic Carbon Nanotube Field-Effect Transistors. *Nature* **2003**, *424*, 654−657.

(2) Franklin, A. D.; Luisier, M.; Han, S.; Tulevski, G.; Breslin, C. M.; Gignac, L.; Lundstrom, M. S.; Haensch, W. Sub-10 nm Carbon Nanotube Transistor. *Nano Lett.* **2012**, *12*, 758−762.

(3) Cao, Q.; Kim, H.; Pimparkar, N.; Kulkarni, J. P.; Wang, C.; Shim, M.; Roy, K.; Alam, M. a; Rogers, J. a. Medium-Scale Carbon Nanotube Thin-Film Integrated Circuits on Flexible Plastic Substrates. *Nature* **2008**, *454*, 495−500.

(4) Izard, N.; Kazaoui, S.; Hata, K.; Okazaki, T.; Saito, T.; Iijima, S.; Minami, N. Semiconductor-Enriched Single Wall Carbon Nanotube Networks Applied to Field Effect Transistors. *Appl. Phys. Lett.* **2008**, *92*, 243112.

(5) Yi, X.; Ozawa, H.; Nakagawa, G.; Fujigaya, T.; Nakashima, N.; Asano, T. Single-Walled Carbon Nanotube Thin Film Transistor Fabricated Using Solution Prepared with 9,9-Dioctyfluorenyl-2,7-diyl−Bipyridine Copolymer. *Jpn. J. Appl. Phys.* **2011**, *50*, 070207.

(6) Star, A.; Han, T.-R.; Joshi, V.; Gabriel, J.-C. P.; Gruner, G. Nanoelectronic Carbon Dioxide Sensors. *Adv. Mater.* **2004**, *16*, 2049−2052.

(7) Snow, E. S.; Perkins, F. K.; Houser, E. J.; Badescu, S. C.; Reinecke, T. L. Chemical Detection with a Single-Walled Carbon Nanotube Capacitor. *Science* **2005**, *307*, 1942−1945.

(8) Wang, C.; Badmaev, A.; Jooyaie, A.; Bao, M.; Wang, K. L.; Galatsis, K.; Zhou, C. Radio Frequency and Linearity Performance of Transistors Using High-Purity Semiconducting Carbon Nanotubes. *ACS Nano* **2011**, *5*, 4169−4176.

(9) Barone, P. W.; Baik, S.; Heller, D. a; Strano, M. S. Near-Infrared Optical Sensors Based on Single-Walled Carbon Nanotubes. *Nat. Mater.* **2005**, *4*, 86−92.

(10) Ding, L.; Tselev, A.; Wang, J.; Yuan, D.; Chu, H.; McNicholas, T. P.; Li, Y.; Liu, J. Selective Growth of Well-Aligned Semiconducting Single-Walled Carbon Nanotubes. *Nano Lett.* **2009**, *9*, 800−805.

(11) Harutyunyan, A. R.; Chen, G.; Paronyan, T. M.; Pigos, E. M.; Kuznetsov, O. a.; Hewaparakrama, K.; Kim, S. M.; Zakharov, D.; Stach, E. a.; Sumanasekera, G. U. Preferential Growth of Single-Walled Carbon Nanotubes with Metallic Conductivity. *Science* **2009**, *326*, 116−120.

(12) Krupke, R.; Hennrich, F.; Löhneysen, H. V.; Kappes, M. M. Separation of Metallic from Semiconducting Single-Walled Carbon Nanotubes. *Science* **2003**, *301*, 344−347.

(13) Krupke, R.; Hennrich, F.; Kappes, M. M.; Lo, H. Surface Conductance Induced Dielectrophoresis of Semiconducting Single-Walled Carbon Nanotubes. *Nano Lett.* **2004**, *4*, 1395−1399.

(14) Krupke, R.; Linden, S.; Rapp, M.; Hennrich, F. Thin Films of Metallic Carbon Nanotubes Prepared by Dielectrophoresis. *Adv. Mater.* **2006**, *18*, 1468−1470.

(15) Tu, X.; Manohar, S.; Jagota, A.; Zheng, M. DNA Sequence Motifs for Structure-Specific Recognition and Separation of Carbon Nanotubes. *Nature* **2009**, *460*, 250−253.

(16) Zheng, M.; Semke, E. D. Enrichment of Single Chirality Carbon Nanotubes. *J. Am. Chem. Soc.* **2007**, *129*, 6084−6085.

(17) Zheng, M.; Jagota, A.; Semke, E. D.; Diner, B. a.; McLean, R. S.; Lustig, S. R.; Richardson, R. E.; Tassi, N. G. DNA-Assisted Dispersion and Separation of Carbon Nanotubes. *Nat. Mater.* **2003**, *2*, 338−342.

(18) Khripin, C. Y.; Fagan, J. a.; Zheng, M. Spontaneous Partition of Carbon Nanotubes in Polymer-Modified Aqueous Phases. *J. Am. Chem. Soc.* **2013**, *135*, 6822−6825.

(19) Nish, A.; Hwang, J.-Y.; Doig, J. Highly Selective Dispersion of Single-Walled Carbon Nanotubes Using Aromatic Polymers. *Nat. Nanotechnol.* **2007**, *2*, 1748−3387.

(20) Mistry, K. S.; Larsen, B. A.; Blackburn, J. L.; Renewable, N.; States, U. High-Yield Dispersions of Single-Walled Carbon Nanotubes with Tunable Narrow Chirality Distributions. *ACS Nano* **2013**, *7*, 2231−2239.

(21) Lee, H. W.; Yoon, Y.; Park, S.; Oh, J. H.; Hong, S.; Liyanage, L. S.; Wang, H.; Morishita, S.; Patil, N.; Park, Y. J.; et al. Selective Dispersion of High Purity Semiconducting Single-Walled Carbon Nanotubes with Regioregular Poly(3-alkylthiophene)s. *Nat. Commun.* **2011**, *2*, 541.

(22) Stranks, S. D.; Baker, A. M. R.; Alexander-Webber, J. a.; Dirks, B.; Nicholas, R. J. Production of High-Purity Single-Chirality Carbon Nanotube Hybrids by Selective Polymer Exchange. *Small* **2013**, *9*, 2245−2249.

(23) Lemasson, F. A.; Strunk, T.; Gerstel, P.; Hennrich, F.; Lebedkin, S.; Barner-kowollik, C.; Wenzel, W.; Kappes, M. M.; Mayor, M. Selective Dispersion of Single-Walled Carbon Nanotubes. *J. Am. Chem. Soc.* **2011**, *133*, 652−655.

(24) Ding, J.; Li, Z.; Lefebvre, J.; Cheng, F.; Dubey, G.; Zou, S.; Finnie, P.; Hrdina, A.; Scoles, L.; Lopinski, G. P.; et al. Enrichment of Large-Diameter Semiconducting SWCNTs by Polyfluorene Extraction for High Network Density Thin Film Transistors. *Nanoscale* **2014**, 2328−2339.

(25) Tange, M.; Okazaki, T.; Iijima, S. Selective Extraction of Large-Diameter Single-Wall Carbon Nanotubes with Specific Chiral Indices by Poly(9,9-dioctylfluorene-alt-benzothiadiazole). *J. Am. Chem. Soc.* **2011**, *133*, 11908−11911.

(26) Moshammer, K.; Hennrich, F.; Kappes, M. M. Selective Suspension in Aqueous Sodium Dodecyl Sulfate According to Electronic Structure Type Allows Simple Separation of Metallic from Semiconducting Single-Walled Carbon Nanotubes. *Nano Res.* **2009**, *2*, 599−606.

(27) Liu, H.; Nishide, D.; Tanaka, T.; Kataura, H. Large-Scale Single-Chirality Separation of Single-Wall Carbon Nanotubes by Simple Gel Chromatography. *Nat. Commun.* **2011**, *2*, 309.

(28) Tanaka, T.; Urabe, Y.; Nishide, D.; Kataura, H. Continuous Separation of Metallic and Semiconducting Carbon Nanotubes Using Agarose Gel. *Appl. Phys. Express* **2009**, *2*, 125002.

(29) Nishide, D.; Liu, H.; Tanaka, T.; Kataura, H. Sorting Single-Wall Carbon Nanotubes Combining Gel Chromatography and Density-Gradient Ultracentrifugation. *Phys. Status Solidi* **2010**, *247*, 2746−2749.

(30) Arnold, M. S.; Stupp, S. I.; Hersam, M. C. Enrichment of Single-Walled Carbon Nanotubes by Diameter in Density Gradients. *Nano Lett.* **2005**, *5*, 713−718.

(31) Arnold, M. S.; Green, A. a.; Hulvat, J. F.; Stupp, S. I.; Hersam, M. C. Sorting Carbon Nanotubes by Electronic Structure Using Density Differentiation. *Nat. Nanotechnol.* **2006**, *1*, 60−65.

(32) Ghosh, S.; Bachilo, S. M.; Weisman, R. B. Advanced Sorting of Single-Walled Carbon Nanotubes by Nonlinear Density-Gradient Ultracentrifugation. *Nat. Nanotechnol.* **2010**, *5*, 443−450.

(33) Green, A. a.; Hersam, M. C. Ultracentrifugation of Single-Walled Nanotubes. *Mater. Today* **2007**, *10*, 59−60.

(34) Wei, L.; Wang, B.; Goh, T. H.; Li, L.-J.; Yang, Y.; Chan-Park, M. B.; Chen, Y. Selective Enrichment of (6,5) and (8,3) Single-Walled Carbon Nanotubes via Cosurfactant Extraction from Narrow (n,m) Distribution Samples. *J. Phys. Chem. B* **2008**, *112*, 2771−2774.

(35) Tanaka, T.; Urabe, Y.; Nishide, D.; Kataura, H. Discovery of Surfactants for Metal/semiconductor Separation of Single-Wall Carbon Nanotubes via High-Throughput Screening. *J. Am. Chem. Soc.* **2011**, *133*, 17610−17613.

(36) Antaris, A. L.; Seo, J. T.; Green, A. A.; Hersam, M. C. Sorting Single Walled Carbon Nanotubes by Electronic Type Using Nonionic, Biocompatible Block Copolymers. *ACS Nano* **2010**, *4*, 4725−4732.

(37) Homenick, C. M.; de Silveira, G.; Sheardown, H.; Adronov, A. Pluronics as Crosslinking Agents for Collagen: Novel Amphiphilic Hydrogels. *Polym. Int.* **2011**, *60*, 458−465.
(38) Homenick, C. M.; Sheardown, H.; Adronov, A. Reinforcement of Collagen with Covalently-Functionalized Single-Walled Carbon Nanotube Crosslinkers. *J. Mater. Chem.* **2010**, *20*, 2887.
(39) Florent, M.; Shvartzman-Cohen, R.; Goldfarb, D.; Yerushalmi-Rozen, R. Self-Assembly of Pluronic Block Copolymers in Aqueous Dispersions of Single-Wall Carbon Nanotubes as Observed by Spin Probe EPR. *Langmuir* **2008**, *24*, 3773−3779.
(40) Arutyunyan, N. R.; Baklashev, D. V.; Obraztsova, E. D. Suspensions of Single-Wall Carbon Nanotubes Stabilized by Pluronic for Biomedical Applications. *Eur. Phys. J. B* **2010**, *75*, 163−166.
(41) Blanch, A. J.; Lenehan, C. E.; Quinton, J. S. Optimizing Surfactant Concentrations for Dispersion of Single-Walled Carbon Nanotubes in Aqueous Solution. *J. Phys. Chem. B* **2010**, *114*, 9805−9811.
(42) Monteiro-Riviere, N. a.; Inman, A. O.; Wang, Y. Y.; Nemanich, R. J. Surfactant Effects on Carbon Nanotube Interactions with Human Keratinocytes. *Nanomedicine* **2005**, *1*, 293−299.
(43) Singh, R. P.; Jain, S.; Ramarao, P. Surfactant-Assisted Dispersion of Carbon Nanotubes: Mechanism of Stabilization and Biocompatibility of the Surfactant. *J. Nanoparticle Res.* **2013**, *15*, 1985.
(44) Antaris, A. L.; Seo, J.-W. T.; Brock, R. E.; Herriman, J. E.; Born, M. J.; Green, A. a.; Hersam, M. C. Probing and Tailoring pH-Dependent Interactions between Block Copolymers and Single-Walled Carbon Nanotubes for Density Gradient Sorting. *J. Phys. Chem. C* **2012**, *116*, 20103−20108.
(45) Yanagi, K.; Iitsuka, T.; Fujii, S.; Kataura, H. Separations of Metallic and Semiconducting Carbon Nanotubes by Using Sucrose as a Gradient Medium. *J. Phys. Chem. C* **2008**, 18889−18894.
(46) Journet, C.; Maser, W. K.; Bernier, P.; Loiseau, A.; Lamy de la Chapelle, M.; Lefrant, S.; Deniard, P.; Lee, R.; Fischer, J. . Large-Scale Production of Single-Walled Carbon Nanotubes by the Electric-Arc Technique. *Nature* **1997**, *388*, 20−22.
(47) Kingston, C. T.; Jakubek, Z. J.; Dénommée, S.; Simard, B. Efficient Laser Synthesis of Single-Walled Carbon Nanotubes through Laser Heating of the Condensing Vaporization Plume. *Carbon (N.Y.)* **2004**, *42*, 1657−1664.
(48) Kim, K. S.; Cota-Sanchez, G.; Kingston, C. T.; Imris, M.; Simard, B.; Soucy, G. Large-Scale Production of Single-Walled Carbon Nanotubes by Induction Thermal Plasma. *J. Phys. D. Appl. Phys.* **2007**, *40*, 2375−2387.
(49) Wang, F.; Sfeir, M.; Huang, L.; Huang, X.; Wu, Y.; Kim, J.; Hone, J.; O'Brien, S.; Brus, L.; Heinz, T. Interactions between Individual Carbon Nanotubes Studied by Rayleigh Scattering Spectroscopy. *Phys. Rev. Lett.* **2006**, *96*, 167401.
(50) Tabakman, S. M.; Welsher, K.; Hong, G.; Dai, H. Optical Properties of Single-Walled Carbon Nanotubes Separated in a Density Gradient; Length, Bundling, and Aromatic Stacking Effects. *J. Phys. Chem. C* **2010**, *114*, 19569−19575.
(51) Naumov, A. V.; Ghosh, S.; Tsyboulski, D. A.; Bachilo, S. M.; Weisman, R. B. Analyzing Absorption Backgrounds in Single-Walled Carbon Nanotube Spectra. *ACS Nano* **2011**, *5*, 1639−1648.
(52) *Surfactants Pluronic & Tetronic*; BASF - The Chemical Company: Florham Park, NJ, USA, 2011, pp 1−37.
(53) Holland, R. J.; Parker, E. J.; Guiney, K.; Zeld, F. R. Fluorescence Probe Studies of Ethylene Oxide/Propylene Oxide Block Copolymers in Aqueous Solution. *J. Phys. Chem.* **1995**, *99*, 11981−11988.
(54) Lopes, J. R.; Loh, W. Investigation of Self-Assembly and Micelle Polarity for a Wide Range of Ethylene Oxide-Propylene Oxide-Ethylene Oxide Block Copolymers in Water. *Langmuir* **1998**, *14*, 750−756.
(55) Itkis, M. E.; Perea, D. E.; Niyogi, S.; Rickard, S. M.; Hamon, M. a.; Hu, H.; Zhao, B.; Haddon, R. C. Purity Evaluation of As-Prepared Single-Walled Carbon Nanotube Soot by Use of Solution-Phase Near-IR Spectroscopy. *Nano Lett.* **2003**, *3*, 309−314.
(56) Green, A. a.; Hersam, M. C. Colored Semitransparent Conductive Coatings Consisting of Monodisperse Metallic Single-Walled Carbon Nanotubes. *Nano Lett.* **2008**, *8*, 1417−1422.
(57) Strano, M. S.; Huffman, C. B.; Moore, V. C.; O'Connell, M. J.; Haroz, E. H.; Hubbard, J.; Miller, M.; Rialon, K.; Kittrell, C.; Ramesh, S.; et al. Reversible, Band-Gap-Selective Protonation of Single-Walled Carbon Nanotubes in Solution. *J. Phys. Chem. B* **2003**, *107*, 6979−6985.
(58) Ramesh, S.; Ericson, L. M.; Davis, V. a.; Saini, R. K.; Kittrell, C.; Pasquali, M.; Billups, W. E.; Adams, W. W.; Hauge, R. H.; Smalley, R. E. Dissolution of Pristine Single Walled Carbon Nanotubes in Superacids by Direct Protonation. *J. Phys. Chem. B* **2004**, *108*, 8794−8798.
(59) Antaris, A. L.; Seo, J. T.; Brock, R. E.; Jane, E.; Born, M. J.; Green, A. A.; Hersam, M. C. Probing and Tailoring pH-Dependent Interactions between Block Copolymers and Single-Walled Carbon Nanotubes for Density Gradient Sorting. *J. Phys. Chem. C* **2012**, *116*, 20103−20108.
(60) Nagarajan, R. Theory of Surfactant Self -Assembly: A Predictive Molecular Thermodynamic Approach. *Langmuir* **1991**, 2934−2969.
(61) *Standard Methods for the Examination of Water and Wastewater*, 12th ed.; American Public Health Association: New York, 1965; pp 408−410.
(62) Gobre, V. V.; Tkatchenko, A. Scaling Laws for van der Waals Interactions in Nanostructured Materials. *Nat. Commun.* **2013**, *4*, 2341.